J Mol Med (2002) 80:524–532
DOI 10.1007/s00109-002-0364-0

ORIGINAL ARTICLE

**Dirk Isbrandt · Patrick Friederich · Anna Solth
Wilhelm Haverkamp · Andreas Ebneth
Martin Borggrefe · Harald Funke · Kathrin Sauter
Günter Breithardt · Olaf Pongs · Eric Schulze-Bahr**

Identification and functional characterization of a novel *KCNE2* (MiRP1) mutation that alters HERG channel kinetics

Received: 18 December 2001 / Accepted: 30 April 2002 / Published online: 28 June 2002

Abstract Long-QT syndrome (LQTS) may cause syncope and sudden death due to cardiac tachyarrhythmia. Chromosome 7-linked LQTS (LQT2) has been correlated with mutations in the human ether-a-go-go-related gene (HERG). HERG forms voltage-gated K channels that may be associated with Mink-related peptide 1 (MiRP1), an auxiliary β-subunit. The channels mediate currents that resemble native I_{Kr}. Mutations in the *KCNE2* gene encoding MiRP1 may also cause LQTS. In this study, the frequency of mutations in *KCNE2* of 150 unrelated LQTS patients without known genotype and of 100 controls was analyzed using single-strand conformation polymorphism analysis and direct sequencing. We identified a novel missense mutation, V65 M, in the *KCNE2* gene of a 17-year-old female with syncope and LQTS. Expression studies in Chinese hamster ovary cells revealed that mutant and wild-type MiRP1 co-localized with HERG subunits and formed functional channels. However, mutant HERG/MiRP1$_{V65M}$ channels mediated currents with an accelerated inactivation time course compared with wild-type channels. The accelerated inactivation time course of HERG/MiRP1$_{V65M}$ channels may decrease I_{Kr} current density of myocardial cells, thereby impairing the ability of myocytes to repolarize in response to sudden membrane depolarizations such as extrasystoles.

Keywords Long QT syndrome · *KCNE2* · MiRP1 · Genetics · Ventricular tachycardia

PATRICK FRIEDERICH works as a specialist anaesthesiologist at the Clinic of Anaesthesiology and Intensive Care Medicine (Director: Prof. J. Schulte am Esch) at the University Hospital in Hamburg, Germany. After graduating from Medical School in Berlin he did his doctoral thesis at the Rheinische-Friedrich-Wilhelms University Bonn on the interaction of general anaesthetic agents with human potassium channels. His current research work focuses on the impact of anaesthetic agents on perioperative morbidity with special reference to inherited and acquired cardiac arrhythmia.

ERIC SCHULZE-BAHR graduated from the Medical School of the University of Göttingen, Germany. He is presently postdoctoral fellow in the Department of Cardiology (Director: Prof. G. Breithardt) at the University of Münster, Germany, and on training for Internal Medicine. His group "Genetics of Arrhythmias" focuses on the molecular genetic basis of cardiac disorders, especially on inherited arrhythmias, and the impact of gene modifiers in inherited and acquired diseases.

Dirk Isbrandt and Patrick Friederich contributed equally to this work

D. Isbrandt (✉) · P. Friederich · A. Solth · K. Sauter · O. Pongs
Institute for Neural Signal Transduction,
Centre for Molecular Neurobiology Hamburg,
University of Hamburg, Martinistrasse 52,
20246 Hamburg, Germany
e-mail: isbrandt@uni-hamburg.de
Tel.: +49-40-428036650
Fax: +49-40-428036643

H. Funke · G. Breithardt · E. Schulze-Bahr
Institute for Arteriosclerosis Research, University of Münster,
Münster, Germany

W. Haverkamp · M. Borggrefe · G. Breithardt · E. Schulze-Bahr
Department of Cardiology, University Hospital,
Münster, Germany

A. Ebneth
GENION Forschungsgesellschaft, Hamburg, Germany

Introduction

The long-QT syndrome (LQTS) is an autosomal dominantly inherited cardiac disorder that is characterized by

a prolonged QT interval. It causes increased susceptibility to ventricular tachyarrhythmias, resulting in syncope and sudden death of otherwise healthy individuals [1, 2].

Five LQTS-associated genes have hitherto been identified. They either encode α-subunits of cardiac ion channels, e.g., the sodium channel gene *SCN5A* (LQTS3) [3], the potassium channel genes *KCNQ1* (LQTS1) [4] and HERG (or *KCNH2*; LQTS2) [5], or the auxiliary K channel ß-subunits MinK (*KCNE1*, LQTS5) [6, 7] and, recently identified, MiRP1 (*KCNE2*) [8]. HERG and MiRP1 co-assemble to form functional channels [8]. Their biophysical and pharmacological properties resemble native channels, conducting the rapidly activating delayed rectifier current I_{Kr} [8]. Both HERG and MiRP1 mutants may affect I_{Kr}. This can lead to delayed myocardial repolarization and thus reduce the individual repolarization reserve [9], thereby conferring increased susceptibility to ventricular tachyarrhythmias.

The *KCNE2* gene encoding MiRP1 is located on chromosome 21q22.1, and its open reading frame is not interrupted by an intron [8]. The deduced MiRP1 protein sequence predicts a small, 123-amino acid protein with one putative membrane-spanning domain, an extracellular N-terminus and an intracellular C-terminus [8]. A few *KCNE2* missense mutations were recently identified in patients with inherited LQTS or drug-induced LQTS [8, 10]. When co-expressed with HERG in heterologous expression systems, the mutant MiRP1 subunits affected I_{Kr}-like K currents, slowed activation, accelerated deactivation, and increased drug sensitivity, respectively [8, 10]. Co-expression of wild-type MiRP1 with HERG subunits carrying mutations in the cyclic nucleotide-binding domain revealed that MiRP1 determined the in vitro phenotype of these mutations [11]. Using in vitro systems it has recently also been shown that MiRP1 has the capability of interacting with KCNQ1 [12], Kv4.2 [13] or HCN1 channels [14], although the physiological significance of these findings remains uncertain.

In this study, we screened the *KCNE2* gene of 150 unrelated LQTS patients without known genotype. Within all known LQTS genes of a 17-year-old female with a history of syncope and a prolonged QTc interval on the surface electrocardiogram (ECG), the only alteration that was identified was a novel missense mutation (V65 M) in the *KCNE2* gene that was detected in a 17-year-old female with a history of syncope and a prolonged QT_c interval on the surface electrocardiogram (ECG). When expressed in Chinese hamster ovary (CHO) cells, mutant MiRP1 co-assembled with HERG in the membrane and formed channels with altered inactivation kinetics, thus providing a possible mechanistic link to the observed clinical phenotype.

Materials and methods

Patients and controls

Venous blood samples of 150 unrelated LQTS patients and of 100 unrelated subjects from the general population with normal QT_c intervals, who served as control group [15], were taken after informed consent had been obtained.

The patient who carried a *KCNE2* mutation was a 17-year-old female, who was admitted to hospital after syncope, which had occurred for the first time in her life. Using 12-lead routine ECG a prolonged QT_c interval was documented (Fig. 1, 480 $ms^{1/2}$, Lead II). During exercise ECG, T-wave alternans occurred. Other cardiac examination revealed no evidence of organic heart disease. There was no family history of sudden cardiac death or symptoms related to familial LQTS. Her asymptomatic mother showed a borderline QT_c interval (460 $ms^{1/2}$) without the above-mentioned alterations in T-wave morphology. Sinus bradycardia (55 bpm), but normal ventricular repolarization (QT_c 360 $ms^{1/2}$) were found on the baseline ECG of the father. Additional family members were not available for analysis.

The study was performed in accordance with the revised forms of the ethical standards laid down in the Declaration of Helsinki (World Medical Association [16]) and with recommendations given by the Ethics Committee of the University of Münster.

Mutational analysis

Genomic DNA was isolated using standard procedures, and PCR was performed as previously reported [15]. In the index patient and her mother, single-strand conformation polymorphism (SSCP) analysis of all exons of the five known LQT genes was performed using previously published primers [7,17, 18. 19, 20] that cover the complete coding sequence and the exon-intron boundaries, including the lariat site. Exon 1 of the *KCNE2* gene was subdivided into three amplicons for SSCP analysis; primers for amplicon 1–1 were CCGTTTTCCTAACCTTGTTCG (sense; sequences are given in 5′–3′ orientation) and AGCATCAACTTTGGCTTGGAG (antisense), for amplicon 1–2 GTCTTCCGAAGGATTTTTATTAC (sense) and GTTCCCGTCTCTTGGATTTCA (antisense), and for amplicon 1–3 AATGTTCTCTTTCATCATCG (sense) and TGTCTGGACGTCAGATGTTAG (antisense). Routine SSCP analysis was performed with Cy5-labelled PCR primers, fluorograms were obtained from an A.L.F. DNA sequencer (Amersham-Pharmacia, Freiburg/Germany). DNA sequencing of PCR-amplified genomic regions was performed when SSCP analysis revealed an abnormally migrating DNA fragment (‘shifted fragment’; in comparison with wild-type conformation, altered fragment mobility during electrophoresis); standard procedures were used [15].

Cloning of MiRP1 expression vector and in vitro mutagenesis

A fragment encoding the complete open reading frame of the *KCNE2* gene was amplified from human genomic DNA by a standard PCR reaction employing *KCNE2*-specific primers. For expression the PCR fragment was subcloned into the mammalian expression vector pcDNA6 (Invitrogen, Groningen, The Netherlands). The amino acid exchange V65M was introduced into *KCNE2* using the quick change site-directed mutagenesis kit (Stratagene, La Jolla, USA) according to the supplier’s instructions with primers *KCNE2*-V65Mc (sense, 5′-CTCTTTCATCATCATGGCCATCCTGGTGA-3′) and *KCNE2*-V65Mnc (antisense, 5′-TCACCAGGATGGCCATGATGATGAAAGAG-3′). Successful mutagenesis and the MiRP1 cDNA sequence were verified by sequencing. In order to facilitate detection of the proteins in immunocytochemical experiments (Fig. 2), N-terminal c-*myc* [21] or C-terminal Flag epitope [22, 23] sequences were introduced into wild-type and mutant *MiRP1* and *HERG*, respectively, using PCR. The sequences of the resulting constructs were also verified by sequencing.

Cell culture, transfection and immunofluorescence of CHO cells

CHO cells or CHO cells stably expressing HERG (carrying a C-terminal Flag tag) were grown in Dulbecco’s modified Eagle’s

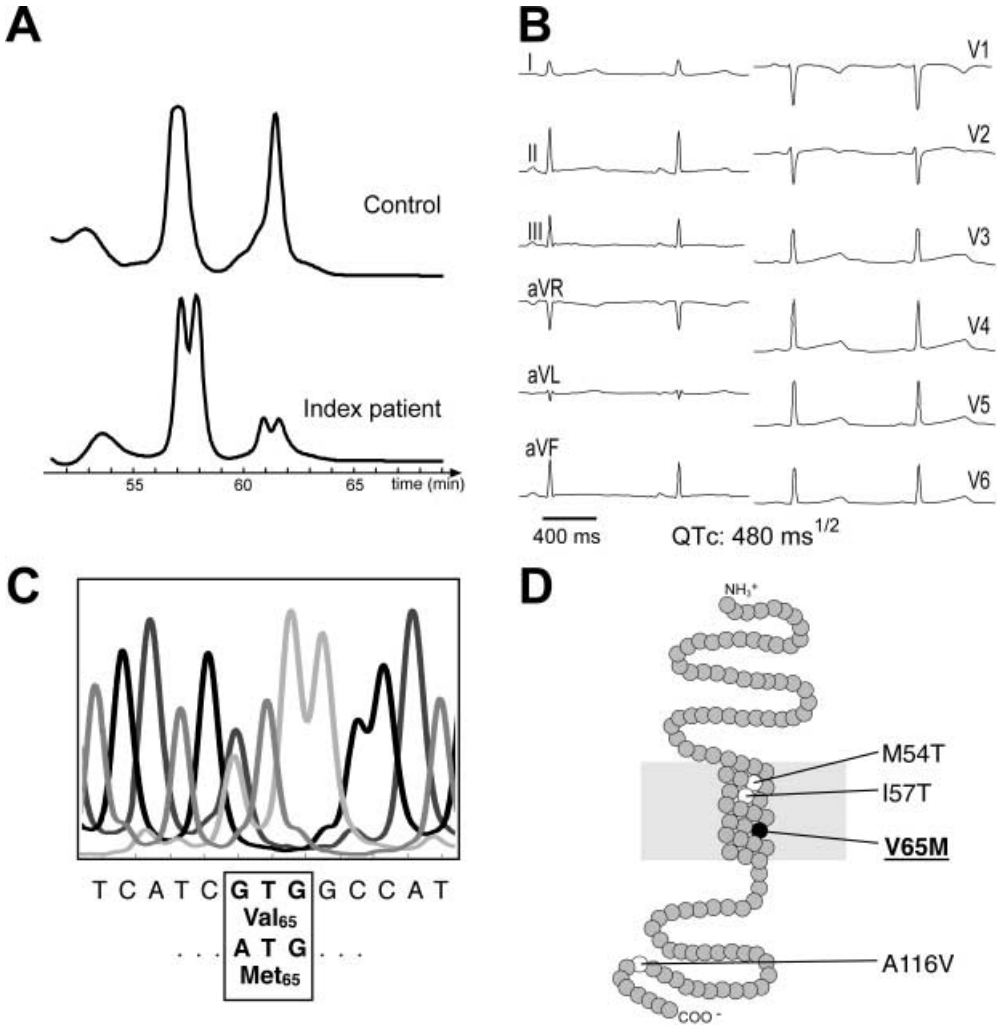

Fig. 1 **A** Fluorograms obtained after single-strand conformation polymorphism (SSCP) analysis of the middle part of exon 1 of the *KCNE2* gene. The wild-type fragment pattern is shown in the *upper panel*; in contrast, a fragment shift (due to an altered electrophoretic mobility) was observed in the index patient (*lower panel*). **B** A 12-lead electrocardiogram (ECG) of the female index patient carrying a *KCNE2* mutation (V65 M) showed a QT_c prolongation (480 $ms^{1/2}$), a depressed T-wave and an ascending ST-segment. **C** Fluorograms obtained after sequencing of amplicon 2 in the *KCNE2* gene containing the middle part of exon 1. Both parental alleles are shown. A heterozygous nucleotide exchange at nucleotide 193 (from G to A) was found corresponding to the amino acid exchange V65 M within the putative transmembranous protein domain of MiRP1. **D** Hitherto identified *KCNE2* mutations associated with inherited LQTS and schematic representation of the predicted membrane topology of MiRP1. The mutation V65 M identified in this study is shown as a *filled circle*, and mutations previously identified by others as *open circles* [8, 10]

Alpha medium supplemented with 10% fetal calf serum (FCS) and antibiotics. The stable HERG cell line was shown to express this channel in every cell analyzed using patch-clamp and immunofluorescence techniques (data not shown). The cells were seeded on coverslips in a 24-multiwell plate 1 day before transfection, which was performed using 3 µl of lipofectamine reagent (Gibco-BRL, Rockville, USA) according to the manufacturer's protocol and 2 µg of the respective MiRP1 plasmid DNA. One day following transfection, cells were fixed on coverslips with 2% paraformaldehyde. After a blocking incubation [1 h at 37°C with 3% goat serum, 5% bovine serum albumin (Sigma, Deisenhoffen, Germany) in phosphate-buffered saline (PBS)], immunostaining was performed with the following antibodies: the affinity-purified anti-myc monoclonal antibody (dilution 1:100; Roche Diagnostics, Mannheim, Germany) and the polyclonal anti-Flag tag antibody (dilution 1:250; Zymed, San Francisco, USA). Secondary reagents for immunofluorescence staining were a Cy2-labelled anti-rabbit IgG (dilution 1:1,000; AP-biotech, Freiburg, Germany) and a Cy3-labelled anti-rabbit IgG (dilution 1:2,000; Mo Bi Tec, Göttingen, Germany). For detection of extracellular myc tags, unfixed cells were incubated successively at 37°C for 1 h with primary and secondary antibodies, which were diluted in fresh medium containing 10% FCS. Cells were washed with PBS and finally fixed with 2% paraformaldehyde. The confocal images were obtained using a Leica TCS NT laser scanning microscope (Leica, Bensheim, Germany).

Whole-cell recordings of CHO cells

Cell culture and transfection of CHO cells for patch-clamp analysis were performed as described above using 1 µg plasmid DNA of HERG (in pcDNA3) and MiRP1 (in pcDNA6), respectively, and 0.5 µg of pEGFP (Clontech).

For experiments shown in Figs. 3C and 4E, a CHO cell line stably expressing HERG was transfected with plasmids (1 µg) encoding either wild-type or mutant MiRP1, respectively, and EGFP, which was coupled to MiRP1 expression by the introduction of the internal ribosomal entry site (IRES) of the polio virus. Transfected cells were identified by EGFP expression. Voltage-sensitive K currents were recorded on the first 2 days after transfection at room temperature (22–25°C) with an EPC-9 amplifier (HEKA Elektronik, Lambrecht, Germany) and Pulse software Version 8.11 (HEKA, Elektronik, Lambrecht, Germany) using the whole-cell patch-clamp technique. Patch electrodes with a pipette resistance between 2 and 4 MΩ were pulled from borosilicate glass capillary tubes (World Precision Instruments, Saratoga, USA) and filled with the following internal solution (mM): KCl 160, $MgCl_2$ 0.5, NaATP 2, HEPES 10, pH 7.2 (with KOH). The extracellular solution contained (mM): NaCl 135, KCl 5, $MgCl_2$ 2, $CaCl_2$ 2, sucrose 10, HEPES 5, pH 7.4 (with NaOH). The capacities of the cells tested did not differ between those expressing HERG/MiRP1 and those expressing HERG/$MiRP1_{V65M}$ channels, and were on average 25 pF. Series resistance was actively compensated. It did not differ between experiments with HERG/MiRP1 and HERG/$MiRP1_{V65M}$ channels and was below 4 MΩ. The holding potential was –80 mV in all experiments.

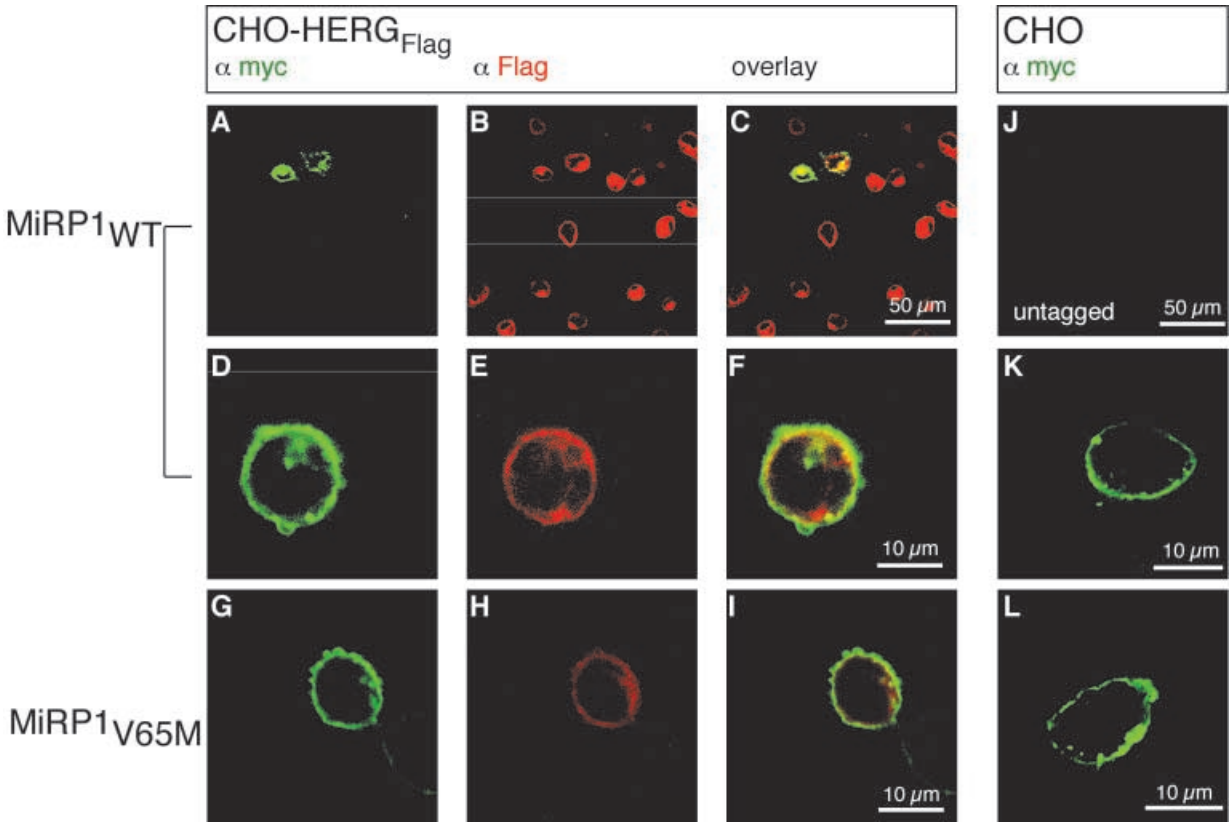

Fig. 2 Surface expression of MiRP1 and MiRP1$_{V65M}$ in the absence and presence of HERG. **A–I** Transient expression of extracellularly myc-tagged wild-type or MiRP1$_{V65M}$, respectively, in Chinese hamster ovary (CHO) cells stably expressing HERG$_{flag}$. **J** Control transfection with untagged MiRP1 expression plasmid. Detection was performed as in **K** and **L**. **K, L** Transient expression of myc-tagged wild-type or MiRP1$_{V65M}$, respectively, in CHO cells in the absence of HERG

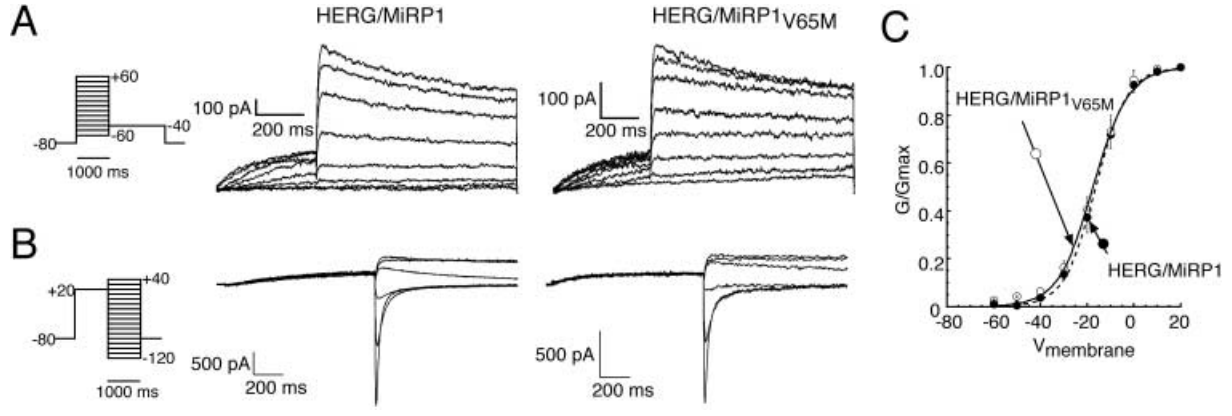

Fig. 3 Current traces of HERG/MiRP1 and HERG/MiRP1$_{V65M}$ channels elicited by the activation (1-s depolarization) (**A)** or by the deactivation (**B)** protocol as shown on the *left*. Using these protocols no significant differences in current densities were observed. **C** Conductance-voltage relationship constructed from the 30-s activation protocol (*closed circles* HERG/MiRP1; *open circles* HERG/MiRP1$_{V65M}$; values are shown as mean±SEM)

Steady-state activation was determined by two-pulse tail current protocols (Figs. 3A and C) with different lengths of the activation step. The membrane was depolarized either for 1 s or 30 s to test potentials between –60 and +60 mV in 10-mV increments to activate the channels (step 1), and it was then stepped for 2 s to –40 mV in order to elicit tail currents (step 2). The voltage dependence of channel activation was assayed by measuring the relative amplitude of the tail current as a function of test potentials in step 1. The activation of channel conductance was fitted with the Boltzmann function: $G(V)/G_{max}=1–1/\{1+\exp[(V_{1/2}–V)/s]\}$. Data are given as mean±SEM.

Deactivation properties of HERG/MiRP1 and HERG/MiRP1$_{V65M}$ currents were investigated after a 1-s depolarizing test pulse to +20 mV by stepping the membrane potential for 1 s to potentials between –120 mV and +40 mV in 20-mV increments (Fig. 3B).

The voltage dependence of steady-state inactivation [24] was measured by a three-step protocol. After a 3-s depolarizing pulse to +20 mV to activate channels (step 1), the membrane potential was stepped for 30 ms to various test voltages (step 2) and then to

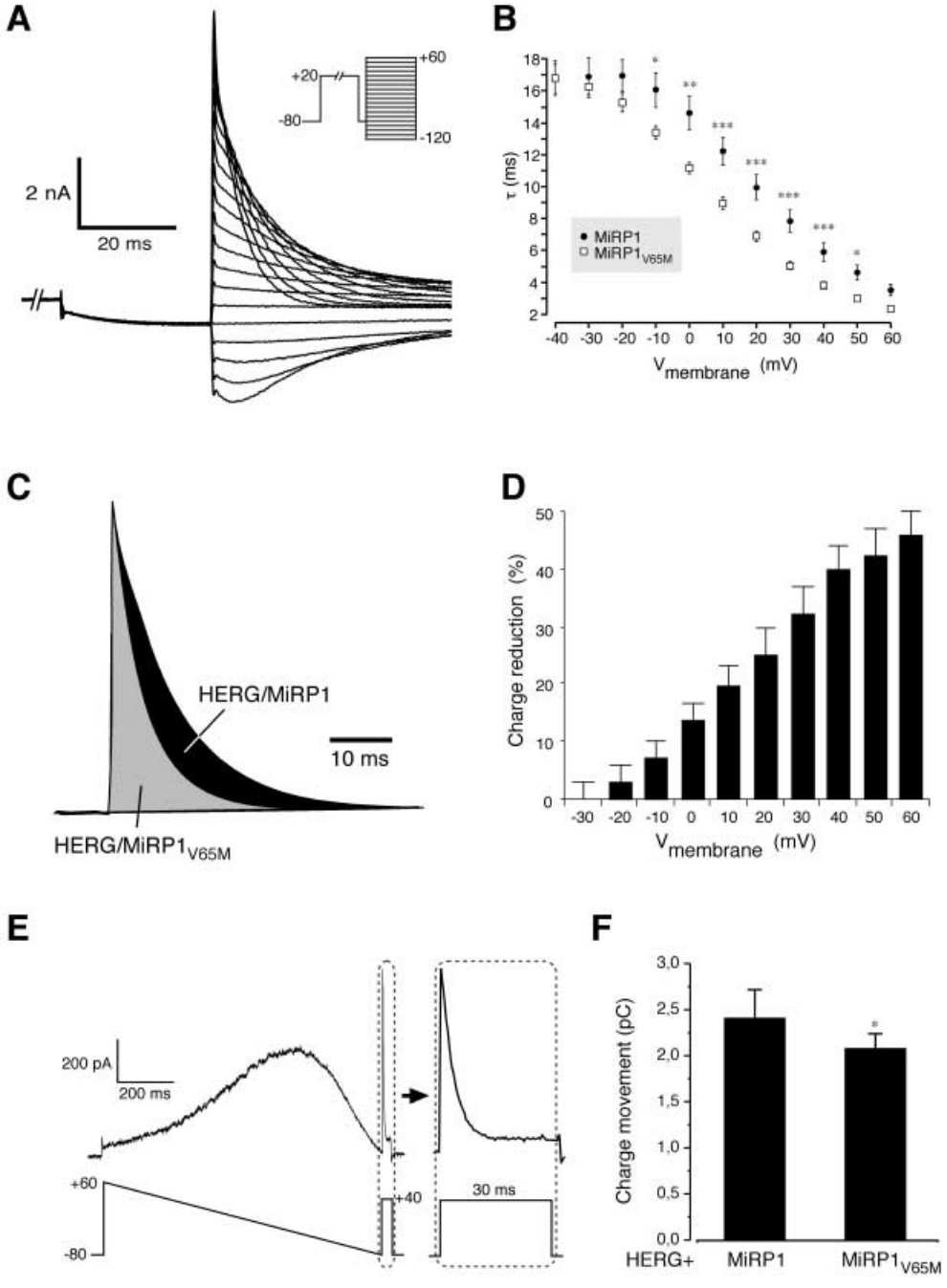

Fig. 4 **A** Current traces of HERG/MiRP1 channels elicited by the instantaneous test protocol as shown in the inset. The currents elicited by the instantaneous inactivation protocol closely resemble I_{Kr} currents in response to extrasystoles. **B** Voltage dependence of inactivation time constants of HERG/MiRP1 and HERG/MiRP1$_{V65M}$ channels (*circles* HERG/MiRP1; *squares* HERG/MiRP1$_{V65M}$, values are shown as mean±SEM). The differences observed were statistically significant between test potentials of –10 and +50 mV (tested with two-way ANOVA for the whole data set (P=0.014) followed by Duncan post test for individual membrane potentials (P=0.021–0.000005). The values ranged from τ=2.3±0.13 to 11.16±0.34 ms (n=10) for mutant and τ=3.52±0.39 ms to 14.61±1.05 ms (n=10) for wild-type HERG/MiRP1 channels. **C** Current traces showing inactivation of HERG/MiRP1 and HERG/MiRP1$_{V65\,M}$ channels at +30 mV. The currents were normalized to the peak current. At +30 mV the inactivation time constants differed significantly (P≤0.01). The areas under the traces in the interval between 2 ms and 30 ms were used to calculate the charge flow across the membrane. **D** Percentage of reduction in K^+ ion flow through mutant I_{Kr} channels. The areas under current traces as shown in **A** and **C** were integrated in the interval between 2 ms and 30 ms. The reduction in charge movement through HERG/MiRP1$_{V65M}$ channels is given as mean±SEM. **E** Representative wild-type HERG/MiRP1 current traces elicited using a modified action potential clamp protocol. The response to the simulated extrasystole is shown enlarged. **F** Charge movement across the membrane in response to the protocol shown in **E** calculated by integrating the area under the current trace between 2 ms and 30 ms. Values are given as mean±SEM; statistical significance is indicated as follows: *P<0.05, **P<0.01, ***P<0.001

a constant membrane potential of +20 mV (step 3). Inactivation was measured as the relative amplitude of the steady-state current in step 3 to the maximum current amplitude in step 2.

The instantaneous current-voltage relationship reflecting the fully activated current [24] was determined as follows: the channels were exposed to a 2-s test potential at +20 mV, then inactivation was removed by stepping the test potential for 30 ms to –80 mV, and currents were elicited for 1 s by the application of test potentials between –120 mV and +60 mV in 10-mV increments (Fig. 4A). The decay of instantaneous currents was used to determine the time constants of inactivation development. Currents were low-pass filtered at 2 kHz and sampled at 6.6 kHz. In order to analyzed differences in charge transfer across the membrane, the areas under the instantaneous current traces between the 2nd and 30th ms were integrated.

A modified ramp protocol was applied for the simulation of an extrasystole following a cardiac action potential. The membrane was depolarized to +60 mV and repolarized within 1 s to the holding potential of –80 mV [25]. Subsequently, the membrane was depolarized for 30 ms to +40 mV. Charge transfer across the membrane was calculated as above.

For graphical representation, current traces were digitally filtered at 400 Hz. A P/4 leak subtraction protocol was used in all protocols except the ramp protocol and the 30-s activation protocol. Statistical analysis was performed with a two-sided heteroscedastic *t*-test (Excel 10, Microsoft, Redmond, USA). For statistical analysis of instantaneous inactivation time constants in Fig. 4B, a two-way repeated measures ANOVA test (between factor: genotype, within factor: membrane potential) with subsequent Duncan post test (Statistica, Statsoft, USA) was applied.

Results

Mutational analysis of the *KCNE2* gene

We screened the *KCNE2* gene of 150 unrelated LQTS patients using SSCP and identified an aberrantly migrating PCR product (Fig. 1A, bottom) in a 17-year-old female presenting with syncope and a prolonged QT_c interval (Fig. 1B). Sequencing of the PCR product revealed a heterozygous nucleotide exchange of nucleotide 193 from G to A in the coding sequence of the *KCNE2* gene (Fig. 1C) that was not present in the *KCNE2* gene of 100 unrelated controls. This mutation results in an amino acid exchange from valine to methionine at position 65 of the MiRP1 protein (Fig. 1C) within the hydrophobic, possibly membrane-spanning segment (Fig. 1D). The other LQT-linked ion channel genes *SCN5A*, *KCNQ1*, *KCNH2* (HERG) and *KCNE1* of this index patient did not have mutations as analyzed by SSCP. The *KCNE2* mutation was verified by sequencing a PCR product amplified from independently prepared genomic DNA of this patient. The analyses of the parents' genotypes showed that the mutation was transmitted by the asymptomatic father, who had a normal resting ECG besides sinus bradycardia. SSCP analysis of all currently known LQT genes revealed no evidence of a LQTS mutation in the mother.

Subcellular localization of HERG and MiRP1 subunits

To assess the expression of wild-type and mutant MiRP1 subunits in transfected CHO cells, HERG α-subunits were tagged with a Flag-tag at the C-terminus and MiRP1 subunits with a myc-tag at the N-terminus. Next, expressed HERG subunits were stained with anti-Flag antibodies and MiRP1 subunits with anti-myc antibodies. The confocal images shown are representative examples of at least ten recorded images per subunit combination, all of which showed comparable staining patterns. Confocal microscopy showed that both the myc-MiRP1 and Flag-HERG immunostaining patterns were concentrated on the cell surface (Figs. 2A–I). The overlapping immunostaining patterns suggested that mutant and wild-type HERG/MiRP1 channels were similarly targeted to the plasma membrane. Interestingly, the myc-MiRP1 immunostaining patterns were similar in the presence (Figs. 2A–I) or absence (Figs. 2K, L) of HERG. This may indicate that the transport of MiRP1 subunits to the CHO cell surface is independent of HERG α-subunit expression. Comparable results have previously been obtained for minK (*KCNE1*) and *KCNE3* subunits [26, 27], respectively.

Table 1 Biophysical properties of HERG/MiRP1 and HERG/$MiRP1_{V65M}$ channels. Values are expressed as mean±SEM. No statistically significant differences were observed (heteroscedastic *t*-test) except for instantaneous inactivation time constants (Fig. 4B, P=0.014, two-way repeated measures ANOVA)

	HERG/MiRP1	$HERG/MiRP_{V65M}$
V_{mid} activation (mV)		
(1 s)	4.6±7.9	0.96±7.0
(30 s)	–16.7±2.5	–17.6±2.2
Slope activation		
(1 s)	8.5±1.0	9.0±2.1
(30 s)	6.6±0.3	7.2±0.7
V_{mid} inactivation (mV)	–60.7±7.43	–60.6±8.31
Slope inactivation	–14.6±2.28	–15.5±1.41
Deactivation $\tau_{-120\ mV}$ (ms)	27±7 and 256±104	28±4 and 224±82
Inactivation $\tau_{+30\ mV}$ (ms)	6.93±2.12	4.92±0.72
P=0.00016[a]		

[a] Duncan post-hoc test

Expression and electrophysiological characterization of wild-type and mutant HERG/MiRP1 channels in CHO cells

Previously, it has been shown that HERG and HERG/MiRP1 channels are less rapidly activated by membrane depolarization than they inactivate when studied in in vitro expression systems [8, 10, 24, 28]. This distinct gating behaviour gives rise to inward rectification, as the channels quickly recover from inactivation at negative potentials and then close slowly to return to the resting, closed state. During this time interval, HERG and HERG/MiRP1 channels may mediate a substantial instantaneous outward current upon renewed depolarization of the membrane by extrasystoles, for example. We used previously developed pulse protocols [24, 28] to

compare the corresponding properties of the currents mediated by HERG/MiRP1 and HERG/MiRP1$_{V65M}$ expressed in CHO cells.

Steady-state activation of HERG/MiRP1 and HERG/MiRP1$_{V65M}$-mediated currents did not differ for the two pulse protocols used (length of the activating pulse 1 s or 30 s, Fig. 3A, C; Table 1). The activation thresholds were at ~–50 mV and currents reached a maximum amplitude at +20 mV. Due to the slow activation kinetics, the voltage of half-maximal activation ($V_{a1/2}$) depended on the length of the activating pulse, as previously reported [29].

The voltage dependence of the inwardly rectifying currents was bell shaped with a maximal current amplitude at –40 to –30 mV. Two deactivation time constants, τ_1 and τ_2 , were fitted to the decay of the inwardly rectifying currents obtained at –120 mV. As summarized in Table 1, they were similar in magnitude and ratio for HERG/MiRP1 [τ_1=27±7 ms and τ_2=256±104 ms (n=6)] and HERG/MiRP1$_{V65M}$ [τ_1=28±4 ms and τ_2=224±82 ms (n=6)], respectively. Similarly, the voltage dependence of steady-state inactivation did not differ between HERG/MiRP1 [$V_{h,1/2}$= –60.7±7.43 mV (slope factor –14.6±2.28, n=7)] and HERG/MiRP1$_{V65M}$ [$V_{h,1/2}$=–60.6± 8.31 mV (slope factor –15.5±1.41, n=6)].

Also, the instantaneous current-voltage relationship was similar for HERG/MiRP1 and HERG/MiRP1$_{V65M}$ (data not shown). In contrast, the HERG/MiRP1$_{V65M}$ currents elicited by the instantaneous current protocol inactivated more rapidly than the HERG/MiRP1 currents (Figs. 4B and C; Table 1). The difference in inactivation time constants was statistically significant between membrane potentials of –10 mV and +50 mV (P≤0.0001–0.03, n=10) (Figs. 4B and C). The voltage dependence of instantaneous inactivation was obviously shifted by ~10 mV to hyperpolarized potentials. The mutation caused a maximum reduction in charge movement across the membrane of 45% (Fig. 4D).

We modified the action potential clamp protocol [25] and added a 30-ms depolarizing test pulse to +40 mV in order to induce currents mediated by HERG/MiRP1 channels similar to currents in response to an extrasystole occurring at the end of the repolarization phase of the action potential (Fig. 4E). No differences in peak current densities were observed between wild-type and mutant I_{Kr} channels (current densities calculated from peak current elicited by the AP clamp protocol: HERG/MiRP1: 34.15±11.3 pA/pF, n=7; HERG/MiRP1$_{V65\ M:}$ 31.01±12.27 pA/pF, n=6; P=0.64). In addition, no significant differences were found in charge movements through wild-type or mutant HERG/MiRP1 channels during the ramp phase of the AP clamp protocol (HERG/MiRP1: 409.86± 238.5 pC; HERG/MiRP1$_{V65\ M}$:432.1±236.7 pC, P=0.87). In agreement with our data obtained with the instantaneous inactivation protocol (Figs. 4A and B), the time course of inactivation was significantly faster for the mutant channels, although to a smaller extent (wt: τ_{+40}=3.3±0.37 ms; mt: τ_{+40}=2.9±0.15 ms; P<0.05). Consequently, charge flow across the cell membrane was diminished in the mutant (Fig. 4F; wt: 2.40±0.36 pC; mt: τ_{+40}=2.09±0.14 pC; P<0.05).

Discussion

To study the frequency of mutations in MiRP1, *KCNE2* was screened in 150 unrelated individuals with LQTS and unknown LQT genotype. Using SSCP and sequence analysis a novel mutation, namely V65 M, was identified and subsequently verified by direct sequencing. The mutation could be detected neither in *KCNE2* of 100 healthy controls nor in the remaining 149 unrelated LQTS patients. Therefore, it is very unlikely that V65 M represents a polymorphism. A comparable frequency of mutations in *KCNE2* was recently reported by Abbott et al. [8], who identified two inherited LQTS-related *KCNE2* mutations in a group of 250 patients. In a recent study, one single nucleotide polymorphism but no mutation were identified by a screen of *KCNE2* in 40 unrelated LQTS patients [30]. These data and our findings collectively suggest that direct involvement of MiRP1 in LQTS is rare.

Our immunocytochemical experiments suggest that the MiRP1 mutation V65 M does not impair protein trafficking when expressed in CHO cells. Apparently, wild-type MiRP1 and MiRP1$_{V65M}$ were correctly targeted to the cell membranes of CHO cells (Figs. 2K and L). When co-expressed with HERG, wild-type or mutant MiRP1 co-localized with HERG at the cell membranes (Figs. 2F and I). In agreement with these observations, HERG/MiRP1$_{V65M}$ formed functional channels in CHO cells comparable to wild-type HERG/MiRP1. Recently, it has been found that a *KCNE2* mutation (M54T) associated with LQTS accelerated deactivation [8]. Channels formed by this mutant had an altered voltage dependence of activation compared with channels formed with wild-type MiRP1. On the other hand, steady-state inactivation was not affected. It was proposed that patients carrying the M54T MiRP1 mutation might have a prolonged QT_c interval because of a decreased I_{Kr} current density. In our case, HERG channels associated with mutant MiRP1$_{V65M}$ had very similar activation, deactivation and steady-state inactivation properties as wild-type channels. A marked difference was observed when the decay of instantaneous currents was measured after recovery of HERG/MiRP1 channels from inactivation or following the simulation of an action potential. In both protocols used, mutant channels inactivated more rapidly than those formed with wild-type HERG/MiRP1 (Figs. 4B, C and F) or HERG alone (data not shown). Thus, the V65 M mutation is not likely to cause a complete loss of MiRP1 function, but rather alters the function of the I_{Kr} channel complex. The conditions under which we produced the instantaneous currents through wild-type and mutant channels simulated those occurring during generation of a premature beat (Figs. 4A and E). Accordingly, a reduction (or diminution) of I_{Kr} activity during an extrasystole might impair the capacity of myocardial cells

to fully repolarize and may thus increase the risk of torsade induction. The analysis of the current flow across the cell membrane in response to the instantaneous pulses, reflecting the capacity of HERG/MiRP1 channels to contribute to repolarization, revealed a significant reduction in charge movement between test potentials of –10 and +50 mV (Fig. 4D, instantaneous inactivation protocol). Furthermore, the time course of instantaneous inactivation of mutant HERG/MiRP1 channels was also significantly accelerated, as was the charge movement through these channels, when we applied the adapted ramp/extrasystole protocol (Figs. 4E and F). In contrast, charge movement during the ramp phase of this protocol, which reflects the I_{Kr} contribution to the repolarization of the normal cardiac action potential, did not differ between wild-type and mutant channels. As a consequence, the MiRP1 mutation should have no or only a slight effect on the action potential duration, as is reflected by the mildly increased QT_c time of the patient's ECG and proposed by a recent publication modelling the effects of mutations in HERG and MiRP1 on the cardiac action potential [31]. Recent studies indicate that MiRP1 may also interact with other ion channels such as KvLQT1, Kv4.2 or HCN4. These results were obtained from in vitro expression systems, and their physiological significance remains uncertain. However, we cannot exclude that the mutant MiRP1 subunit may also interfere with these channels or even affect other, hitherto unknown MiRP1-regulated cellular processes not replicated in the heterologous expression system, which may also contribute to arrhythmogenesis. In addition, the effect of the V65 M mutation in the heterozygous state is hard to predict and was not addressed in our experiments, since the expression system does not provide exact control over the stoichiometry of the expressed subunits.

In the majority of patients with mutations in the *KCNE1* and *KCNE2* genes, a less severe clinical course and incomplete penetrance has been noted so far [6, 8, 32, 33]. *KCNE1* mutations have been associated with autosomal recessive LQTS (Jervell and Lange-Nielsen syndrome, together with inner ear deafness) where the patients' parents are clinically unaffected obligate mutation carriers [7]. In our case, the *KCNE2* mutation was inherited from the asymptomatic father, who had a normal QT_c interval. Recent findings reporting age-gender influences on QT_c, both in normal individuals and in patients with mutations in HERG or *KCNQ1*, respectively, showed that men generally exhibit shorter mean QT_c values than women and thus a lower propensity towards torsade de pointes [34], which may provide an explanation why the father did not show symptoms of LQTS. Extended SSCP analysis of all known LQT genes revealed no evidence of a mutation in the mother, who showed a borderline QT_c of 460 $ms^{1/2}$ and had no history of arrhythmia or syncope. Thus, environmental or genetic factors may influence myocardial repolarization in both mother and daughter, but only the daughter became symptomatic due to a possible synergistic effect of the V65 M mutation in the *KCNE2* gene.

In summary, we identified a novel mutation in the *KCNE2* gene that is associated with inherited LQTS. It causes a change in the inactivation properties of heterologously expressed I_{Kr} channels. The mutation may thus impair an important physiological function of I_{Kr} ion channels, namely the repression of extrasystoles in myocardial cells of the human ventricle.

Acknowledgements The authors are indebted to all persons who participated in this study. We thank E. Morhofer, M. Hesse, K. Alm, A. Schneider-Darlison and A. Zaisser for excellent technical assistance and F. Morellini for help with the statistical analyses. The study was supported by grants from the Foundation Leducq, France; the Deutsche Forschungsgemeinschaft (Schu 1082/2–2, SFB556-A1), Bonn, Germany; the 'Innovative Medizinische Forschung' (Sc1–1-II/97–15) of the University of Münster, Germany; the Franz-Loogen-Foundation, Düsseldorf, Germany; the Alfried Krupp von Bohlen und Halbach-Stiftung, Essen, Germany; and BONFOR of the University of Bonn (PF, O-117.0005).

References

1. Priori SG, Barhanin J, Hauer RN, Haverkamp W, Jongsma HJ, Kleber AG, McKenna WJ, Roden DM, Rudy Y, Schwartz K, Schwartz PJ, Towbin JA, Wilde AM (1999) Genetic and molecular basis of cardiac arrhythmias: impact on clinical management. I, II. Circulation 99:518–528
2. Wang Q, Bowles NE, Towbin JA (1998) The molecular basis of long QT syndrome and prospects for therapy. Mol Med Today 4:382–388
3. Wang Q, Shen J, Splawski I, Atkinson D, Li Z, Robinson JL, Moss AJ, Towbin JA, Keating MT (1995) SCN5A mutations associated with an inherited cardiac arrhythmia, long QT syndrome. Cell 80:805–811
4. Wang Q, Curran ME, Splawski I, Burn TC, Millholland JM, VanRaay TJ, Shen J, Timothy KW, Vincent GM, Jager T de, Schwartz PJ, Toubin JA, Moss AJ, Atkinson DL, Landes GM, Connors TD, Keating MT (1996) Positional cloning of a novel potassium channel gene: *KVLQT1* mutations cause cardiac arrhythmias. Nat Genet 12:17–23
5. Curran ME, Splawski I, Timothy KW, Vincent GM, Green ED, Keating MT (1995) A molecular basis for cardiac arrhythmia: HERG mutations cause long QT syndrome. Cell 80:795–803
6. Splawski I, Tristani-Firouzi M, Lehmann MH, Sanguinetti MC, Keating MT (1997) Mutations in the hminK gene cause long QT syndrome and suppress I_{Ks} function. Nat Genet 17:338–340
7. Schulze-Bahr E, Wang Q, Wedekind H, Haverkamp W, Chen Q, Sun Y, Rubie C, Hördt M, Towbin JA, Borggrefe M, Assmann G, Qu X, Somberg JC, Breithardt G, Oberti C, Funke H (1997) KCNE1 mutations cause Jervell and Lange-Nielsen syndrome. Nat Genet 17:267–268
8. Abbott GW, Sesti F, Splawski I, Buck ME, Lehmann MH, Timothy KW, Keating MT, Goldstein SA (1999) MiRP1 forms IKr potassium channels with HERG and is associated with cardiac arrhythmia. Cell 97:175–187
9. Roden DM (1998) Taking the "idio" out of "idiosyncratic": predicting torsades de pointes. Pacing Clin Electrophysiol 21:1029–1034
10. Sesti F, Abbott GW, Wei J, Murray KT, Saksena S, Schwartz PJ, Priori SG, Roden DM, George AL Jr, Goldstein SA (2000) A common polymorphism associated with antibiotic-induced cardiac arrhythmia. Proc Natl Acad Sci USA 97:10613–10618
11. Cui J, Kagan A, Qin D, Mathew J, Melman YF, McDonald TV (2001) Analysis of the cyclic nucleotide binding domain of the HERG potassium channel and interactions with KCNE2. J Biol Chem 276:17244–17251

12. Tinel N, Diochot S, Borsotto M, Lazdunski M, Barhanin J (2000) KCNE2 confers background current characteristics to the cardiac KCNQ1 potassium channel. EMBO J 19:6326–6330
13. Zhang M, Jiang M, Tseng GN (2001) minK-related peptide 1 associates with Kv4.2 and modulates its gating function: potential role as beta subunit of cardiac transient outward channel? Circ Res 88:1012–1019
14. Yu H, Wu J, Potapova I, Wymore RT, Holmes B, Zuckerman J, Pan Z, Wang H, Shi W, Robinson RB, El-Maghrabi MR, Benjamin W, Dixon J, McKinnon D, Cohen IS, Wymore R (2001) MinK-related peptide 1: a beta subunit for the HCN ion channel subunit family enhances expression and speeds activation. Circ Res 88:E84–E87
15. Schulze-Bahr E, Haverkamp W, Wiebusch H, Schulte H, Hordt M, Borggrefe M, Breithardt G, Assmann G, Funke H (1995) Molecular analysis at the Harvey Ras-1 gene in patients with long QT syndrome. J Mol Med 73:565–569
16. World Medical Association Declaration of Helsinki (1997) Recommendations guiding physicians in biomedical research involving human subjects. Cardiovasc Res 35:2–3
17. Berthet M, Denjoy I, Donger C, Demay L, Hammoude H, Klug D, Schulze-Bahr E, Richard P, Funke H, Schwartz K, Coumel P, Hainque B, Guicheney P (1999) C-terminal HERG mutations: the role of hypokalemia and a KCNQ1-associated mutation in cardiac event occurrence. Circulation 99:1464–1470
18. Neyroud N, Richard P, Vignier N, Donger C, Denjoy I, Demay L, Shkolnikova M, Pesce R, Chevalier P, Hainque B, Coumel P, Schwartz K, Guicheney P (1999) Genomic organization of the KCNQ1 K^+ channel gene and identification of C-terminal mutations in the long-QT syndrome. Circ Res 84:290–297
19. Schulze-Bahr E, Haverkamp W, Wedekind H, Rubie C, Hordt M, Borggrefe M, Assmann G, Breithardt G, Funke H (1997) Autosomal recessive long-QT syndrome (Jervell Lange-Nielsen syndrome) is genetically heterogeneous. Hum Genet 100:573–576
20. Wang Q, Li Z, Shen J, Keating MT (1996) Genomic organization of the human *SCN5A* gene encoding the cardiac sodium channel. Genomics 34:9–16
21. Evan GI, Lewis GK, Ramsay G, Bishop JM (1985) Isolation of monoclonal antibodies specific for human c-*myc* proto-oncogene product. Mol Cell Biol 5:3610–3616
22. Zaidi SH, Hui CC, Cheah AY, You XM, Husain M, Rabinovitch M (1999) Targeted overexpression of elafin protects mice against cardiac dysfunction and mortality following viral myocarditis. J Clin Invest 103:1211–1219
23. Tsiokas L, Arnould T, Zhu C, Kim E, Walz G, Sukhatme VP (1999) Specific association of the gene product of PKD2 with the TRPC1 channel. Proc Natl Acad Sci U S A 96:3934–3939
24. Smith PL, Baukrowitz T, Yellen G (1996) The inward rectification mechanism of the HERG cardiac potassium channel. Nature 379:833–836
25. Hancox JC, Levi AJ, Witchel HJ (1998) Time course and voltage dependence of expressed HERG current compared with native "rapid" delayed rectifier K current during the cardiac ventricular action potential. Pflugers Arch 436:843–853
26. Bianchi L, Shen Z, Dennis AT, Priori SG, Napolitano C, Ronchetti E, Bryskin R, Schwartz PJ, Brown AM (1999) Cellular dysfunction of LQT5-minK mutants: abnormalities of I_{Ks}, I_{Kr} and trafficking in long QT syndrome. Hum Mol Genet 8:1499–1507
27. Schroeder BC, Waldegger S, Fehr S, Bleich M, Warth R, Greger R, Jentsch TJ (2000) A constitutively open potassium channel formed by KCNQ1 and KCNE3. Nature 403:196–199
28. Chen J, Zou A, Splawski I, Keating MT, Sanguinetti MC (1999) Long QT syndrome-associated mutations in the Per-Arnt-Sim (PAS) domain of HERG potassium channels accelerate channel deactivation. J Biol Chem 274:10113–10118
29. Schonherr R, Rosati B, Hehl S, Rao VG, Arcangeli A, Olivotto M, Heinemann SH, Wanke E (1999) Functional role of the slow activation property of ERG K+ channels. Eur J Neurosci 11:753–760
30. Larsen LA, Andersen PS, Kanters J, Svendsen IH, Jacobsen JR, Vuust J, Wettrell G, Tranebjaerg L, Bathen J, Christiansen M (2001) Screening for mutations and polymorphisms in the genes KCNH2 and KCNE2 encoding the cardiac HERG/MiRP1 ion channel: implications for acquired and congenital long Q-T syndrome. Clin Chem 47:1390–1395
31. Mazhari R, Greenstein JL, Winslow RL, Marban E, Nuss HB (2001) Molecular interactions between two long-QT syndrome gene products, HERG and KCNE2, rationalized by in vitro and in silico analysis. Circ Res 89:33–38
32. Schulze-Bahr E, Schwarz M, Hoffmann S, Wedekind H, Funke H, Haverkamp W, Breithardt G, Pongs O, Isbrandt D (2001) A novel long-QT 5 gene mutation in the C-terminus (V109I) is associated with a mild phenotype. J Mol Med 79:504–509
33. Duggal P, Vesely MR, Wattanasirichaigoon D, Villafane J, Kaushik V, Beggs AH (1998) Mutation of the gene for IsK associated with both Jervel l and Lange-Nielsen and Romano-Ward forms of long-QT syndrome. Circulation 97:142–146
34. Lehmann MH, Timothy KW, Frankovich D, Fromm BS, Keating M, Locati EH, Taggart RT, Towbin JA, Moss AJ, Schwartz PJ, Vincent GM (1997) Age-gender influence on the rate-corrected QT interval and the QT-heart rate relation in families with genotypically characterized long QT syndrome. J Am Coll Cardiol 29:93–99